PROGRESSIVE FAILURE ANALYSIS IN POST-BUCKLED CFRP STIFFENED PANEL UNDER COMPRESSION

N.Bouslama[1], A. Maslouhi[1], P.Masson[1] and S.Jazouli[2]
[1]Department of Mechanical Engineering, Université de Sherbrooke /2500, boul. de l'Université, Sherbrooke (Québec) Canada J1K 2R1
Email: Nidhal.Bouslama@Usherbrooke.ca
Email: Ahmed.Maslouhi@usherbrooke.ca, Web Page: http:// http://www.usherbrooke.ca/gmecanique/
[2]Aerostructure and Engineering, Bombardier Aerospace/ 1800 Blvd Marcel Laurin, Montreal (Québec) Canada H4R1K2

Keywords: Composite stiffened panel, buckling, post buckling, progressive damage model, damage tolerance, USERMAT subroutine.

Abstract

Composite materials are now used in the manufacture of efficient aerospace structures as they outperform conventional engineering materials in applications where high specific strength and stiffness are required. Among the main configurations used, stiffened panels are employed in fuselage and wings design. However, in post buckling regime, they exhibit a multitude of damage modes and nonlinear behavior, which require further insight. In this paper, the response of stiffened panels undergoing a static compression load is investigated. A finite-element model is developed based on progressive failure analysis (PFA) and using ANSYS USERMAT subroutine. The damage model was, firstly, compared with experimental results related to simple plate with hole and one single stiffener panel before being applied to two stringers panel. The proposed model shows ability to predict correctly the final strength and to follow main damage modes involved during compression process.

1. Introduction

Advanced composite materials like carbon fiber-reinforced polymer (CFRP) offer high potential in terms of weight saving and mechanical properties enhancement. Thanks to these advantages, CFRP is actually widely introduced in the fabrication of principal structure elements (PSE) like wings, fuselage and rudder. On the other hand, the recourse to composite material raises new issues related to their design and behavior during in service life. Indeed, the anisotropic and heterogeneous nature of this material promotes various and complex failure modes, which did not exist before with conventional isotropic metal alloys. Fiber misalignment, micro buckling, matrix cracking and shear failure are the main damage mechanism observed under compressing loading. These micro damage promote interlaminar disbond and initiate delamination defects between adjacent plies. Delamination was identified in several studies [1-2] as the main common failure mechanism in laminates and may result in important stiffness degradation even for non-visible defects [2]. Therefore, it is crucial to develop adapted analytical and predictive tools taking into account the damage onset and propagation in the early phases of design.

In this study buckling and post-buckling response of stiffened panel is investigated under compression loading. In general, the stiffened panel structures used in fuselages and wings, are sensitive to buckling failure under plane loads. These structures can still carry load even after the appearance of the first

Excerpt from ISBN 978-3-00-053387-7

buckling signs. In the post-buckling regime, large skin deflections are observed while the stringer remains straight and supports the main part of loading. Taking advantage of this phase means to be able to predict complex non-linear response and take into account the interaction between the different failure modes involved throughout this process. In last few years, several studies were conducted to characterize damage tolerance in composite stiffened panel [1-3]. Although, experimental trials emphasize that the skin-stiffener separation is the main failure mode during buckling phase, the final failure is characterized by the stringer collapse.

Recently, it has become possible to predict damage onset and spread using finite element model in large scale structures. These achievement were made thanks to advanced simulation tools based on linear fracture and damage mechanics [4]. Among the most relevant techniques, one can cite; the virtual crack closure technique (VCCT) [4], the cohesive zone modeling CZM [5] and progressive damage technique which will be used in this study.

2. Progressive damage methodology and failure criteria definition

Progressive failure analysis (PFA) is one of the most efficient tools for damage modeling. This technique offers the possibility to predict damage propagation paths and damage modes based on failure criteria and stress distribution. The principle behind this approach consists in applying a degradation factor and reduce the stiffness of damaged elements following a predefined degradation law. The use of a degradation rule allows to monitor damage progression and count its effects via updating consistently the stiffness matrix.

This method has been successfully implemented in numerous studies where different geometries and loading cases were applied; Chang [6] was among the first, to use this approach on simple 2D laminated plate containing a stress concentration site, then compare analytical strength prediction to numerical one. Shokrieh and Lessard [7] used PFA to predict failure in bolted laminate composite subjected to compressive loading. Olmedo [8] expanded Chang-Lessard criteria by introducing out of plane stress to simulate the damage scenarios in hybrid lap joint.

In literature, different failure criteria are proposed to predict damage modes in laminate structures. The most common used criteria are Hashin [9], Puck [10] and LARC04 [11]. In each criterion, analytic expression related to matrix cracks, fiber breakage and interlaminar defects are defined.

For this study, failure criteria proposed by Olmedo [8] and based on Chang-Chang [6] and Shokrieh-Lessard [7] development are used. These criteria combine both the contribution of out of plane stress and the nonlinear shear stress-strain relationship which is expressed by equation (eq.1).

$$\gamma_{12} = \frac{1}{G_{12}}\,\tau_{12} + \alpha\tau_{12}^3 \qquad (1)$$

where γ and τ are respectively the strain and stress field and α is an experimental parameter [12].

The adopted failure criteria are expressed by equations (eq.2-4):

1) Fiber failure:

Fiber failure criteria take into account the interaction between longitudinal stress, in-plane and out of plane shear stress. The failure occurs when the following criterion is satisfied:

$$\sqrt{\left(\frac{\sigma_{11}}{X_T}\right)^2 + \frac{\frac{\tau_{12}^2}{G_{12}^2} + \frac{3}{4}\,\alpha\tau_{12}^4}{\frac{S_{12}^2}{2G_{12}^2} + \frac{3}{4}\,\alpha S_{12}^4} + \frac{\frac{\tau_{13}^2}{G_{13}^2} + \frac{3}{4}\,\alpha\tau_{13}^4}{\frac{S_{13}^2}{2G_{13}^2} + \frac{3}{4}\,\alpha S_{13}^4}} = 1 \qquad \sigma_{11} > 0 \qquad (2)$$

Excerpt from ISBN 978-3-00-053387-7

where X_T is replaced by X_c if $\sigma_{11} < 0$. Here S_{13} and S_{23} are the out-of-plane shear strength.

2) Matrix failure:

In addition to transverse and in plane shear stress, the following failure criterion also considers the contribution of out-of-plane shear stress.

$$\sqrt{(\frac{\sigma_{22}}{Y_T})^2 + \frac{\frac{\tau_{12}^2}{2G_{12}^2} + \frac{3}{4}\,\alpha\tau_{12}^4}{\frac{S_{12}^2}{2G_{12}^2} + \frac{3}{4}\,\alpha S_{12}^4} + \frac{\frac{\tau_{23}^2}{G_{23}^2} + \frac{3}{4}\,\alpha\tau_{23}^4}{\frac{S_{23}^2}{2G_{23}^2} + \frac{3}{4}\,\alpha S_{23}^4}} = 1 \qquad \sigma_{22} > 0 \tag{3}$$

where Y_T is replaced by Y_c if $\sigma_{22} < 0$.

3) Delamination

Delamination criterion used in this study is provided by the expansion of the Hashin criterion and considering the non-linear shear stress/strain behavior. The equation is given by

$$\sqrt{(\frac{\sigma_{33}}{Z_T})^2 + \frac{\frac{\tau_{13}^2}{2G_{13}^2} + \frac{3}{4}\,\alpha\tau_{13}^4}{\frac{S_{13}^2}{2G_{13}^2} + \frac{3}{4}\,\alpha S_{13}^4} + \frac{\frac{\tau_{23}^2}{G_{23}^2} + \frac{3}{4}\,\alpha\tau_{23}^4}{\frac{S_{23}^2}{2G_{23}^2} + \frac{3}{4}\,\alpha S_{23}^4}} = 1 \qquad \sigma_{33} > 0 \tag{4}$$

where Z_T is replaced by Z_c if $\sigma_{33} < 0$.

As failure occurs in a ply of the laminate, the mechanical properties of each material integration point are updated using appropriate degradation parameters as defined in table (1).

Table 1. Degradation rules in different failure modes [13].

Failure mode	E_x	E_y	E_z	G_{xy}	G_{yz}	G_{xz}	υ_{xy}	υ_{yz}	υ_{xz}
Fiber failure	0.14	0.4	0.4	0.25	0.35	0.2	0	0	0
Matrix failure		0.4	0.4	-	-	-	0	0	0
Delamination		0.4	0.4	-	0.2	-	0	0	0

3. USERMAT subroutine and finite element modeling

The progressive damage model defined in previous section has been implemented in ANSYS software using USERMAT subroutine. This approach is deemed advantageous as propose an in-core program far more efficient in term of time computing and result extraction compared to traditional post-processing routine [13]. Compiling the Fortran USERMAT generates an executable file which is called by ANSYS during solution iteration. This custom subroutine requires, firstly, to establish the constitutive material law between stress and strain field by defining the Jacobin matrix $\frac{\partial\sigma}{\partial\varepsilon}$. Subsequently, for every loading step, the program uses the strain increment to compute the corresponding stress field. Thereafter, the program checks if one of the failure criteria is fulfilled, if it's true, an instantaneous degradation is applied according to the values in (Table 1) and new mechanical properties are defined. For each material integration point the updated properties are stored using state variables at the end of time or load increment.

Excerpt from ISBN 978-3-00-053387-7

Updating the stiffness parameters in the global coordinate system, according to the laminate staking sequence is performed automatically in ANSYS (outside of the USERMAT). In this study, all finite element simulations are performed using 3D layered SOLID 286 element with 20 nodes. These elements provide better assessment of interlaminar stress and offer the possibility to store and show results related to each layer.

4. Model validation

A CFRP test plate with a central hole, proposed by Pietropaoli [13] and a single stiffened panel buckling and post-buckling investigation provided by Bisagni [3] were two test cases used in order to validate the methodology suggested in this paper.

4.1. Plate with hole under compression loading

In this section, laminated plate containing a circular hole located at the center is modeled. The specimen has 118x38x1.1mm dimensions and $[-45/90/45/0]_S$ stacking with the same material properties as provided in [13]. The plate was modeled in compression using the damage progressive model defined in the previous section until final collapse and the obtained results in terms of load vs displacement curves are illustrated in (fig. 1). Experimental and numerical results exhibit an excellent correlation: the curve slope and the final failure load fit well. In addition, the model demonstrates its ability to predict correctly the deviation from linearity observed around 19 KN.
The damage evolution maps obtained using state variable are presented in (fig. 2). The graph shows respectively: fiber, matrix and delamination spread before the final failure. Here, the red area illustrates the zone where the corresponding failure criteria is completely fulfilled; failure index is equal to 1. Figure 2, also displays C-Scan map of the damaged area performed by [13] after the final failure, comparable extension area is observed between delamination criterion and inspection results. We can also notice that the final failure was observed when fibers parallel to applied load breaks throw the plate width. This step is also accompanied with numerical convergence difficulties due to highly distorted elements on both sides of the hole.

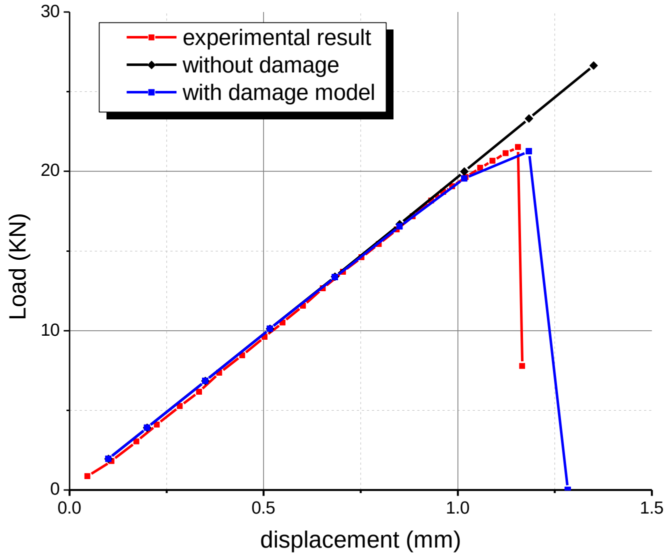

Figure 1. Applied load vs displacement cures.

Excerpt from ISBN 978-3-00-053387-7

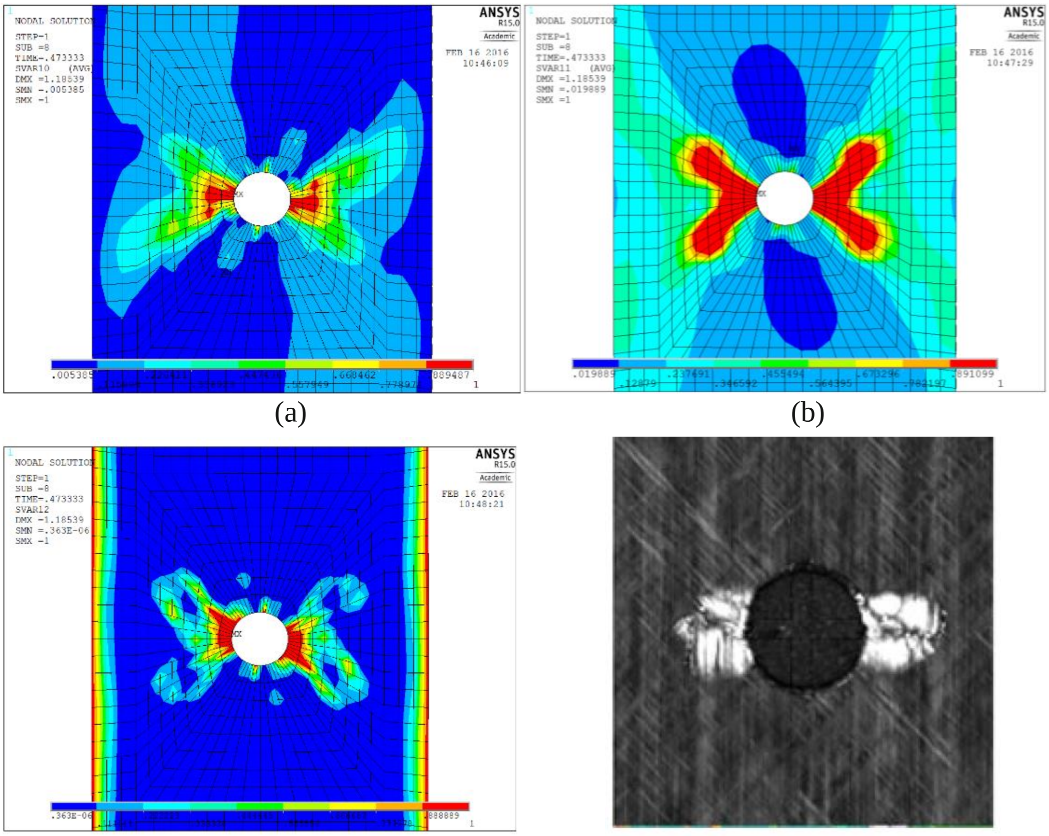

(a) (b)

(c) (d)

Figure 2. Damage map for respectively: (a) fiber breakage, (b) matrix crack, (c) delamination and (d) C-Scan result [13].

4.2. Investigation of damage mode in single stringer stiffened panel under compression loading

The efficiency of USERMAT as in-core program offers the possibility to study a large scale structure without computation time compromises, especially when compared to classic simulation methods. In this section validation process was conducted on one single hat-stiffener panel, and results were compared to experimental one provided in [3]. In addition, the virtual crack closure technique VCCT based on displacements and reaction forces from FE results to compute strain energy release rates, was implemented along the flange tip to supply the mode separation required when using a mixed mode fracture criterion.

The studied model is made from IM7/8552 graphite-epoxy material and have the following dimension; 240mm length, 123mm width and 30mm stringer height. The layup sequences respectively for the skin and the flange are defined as follow: $[-45/90/-45/0]_s$, [-45/0/45/0/45/0/-45].

Load-displacement curves presented in (fig. 3) compare experimental and numerical obtained results. The figure shows similar slope in the linear parts until 10 KN which correspond to the apparition of the first buckling mode. Beyond this value and until the final failure load the FE model exhibits softer behavior. This difference could be explained by geometry variation in modeling especially in stiffener corners which are considered as a resin rich area. The skin-stiffener interface behavior could also affect global behavior and causes some numerical inaccuracies.

Excerpt from ISBN 978-3-00-053387-7

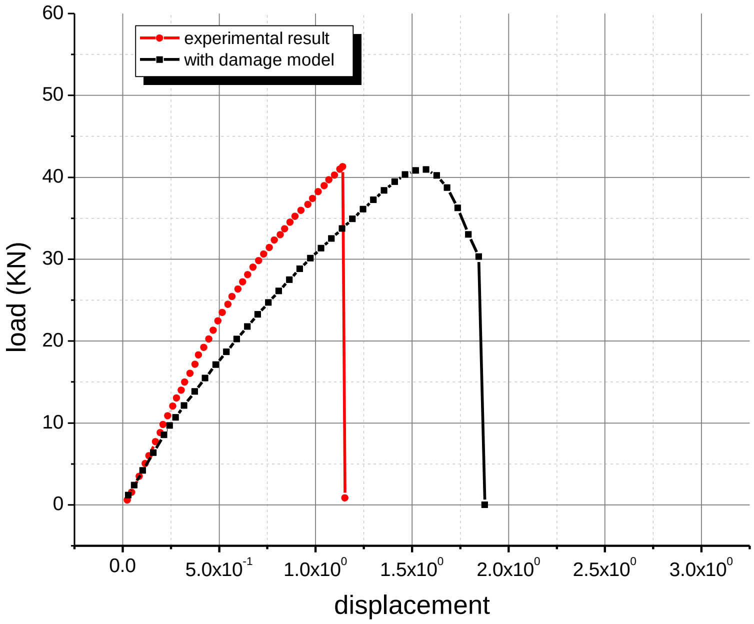

Figure 3. Applied load vs displacement curves

The damage progressive results shown in (fig. 4), highlight the presence of two hot spots corresponding to the area at the maximum out of plane displacement. Indeed, the damage starts at the flange end and located in the interface with the skin. The loading sequences show that delamination was the first criterion to be satisfied closely followed by matrix cracking and fiber breakage. In this case, the damage spreads through the flange from the both sides reaching the top of the stringer before the final failure. The damage map related to three major damage mode prior to the final collapse are illustrated in (fig.4).

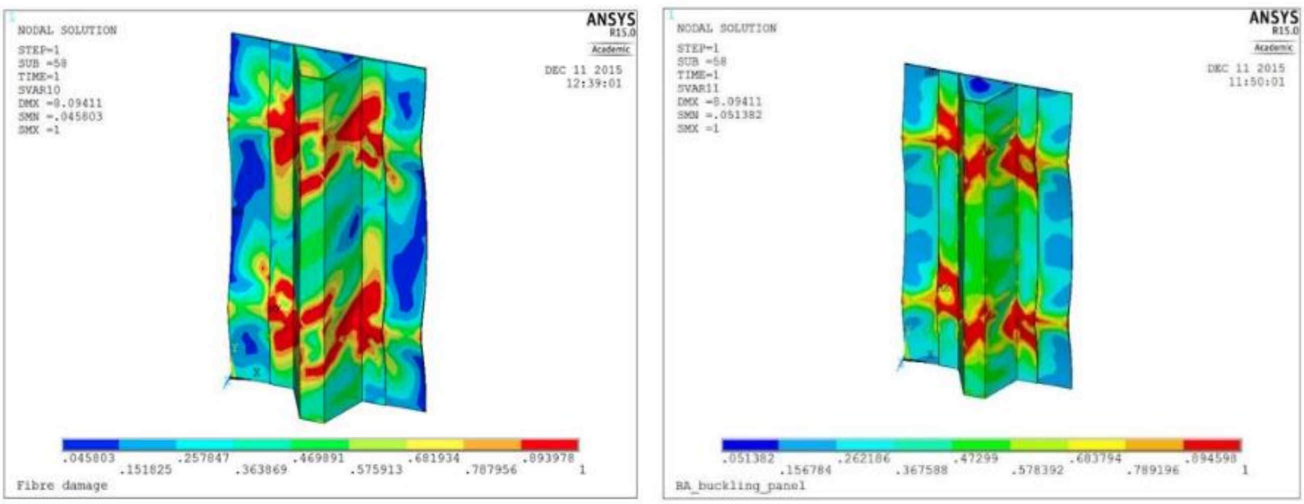

(a) (b)

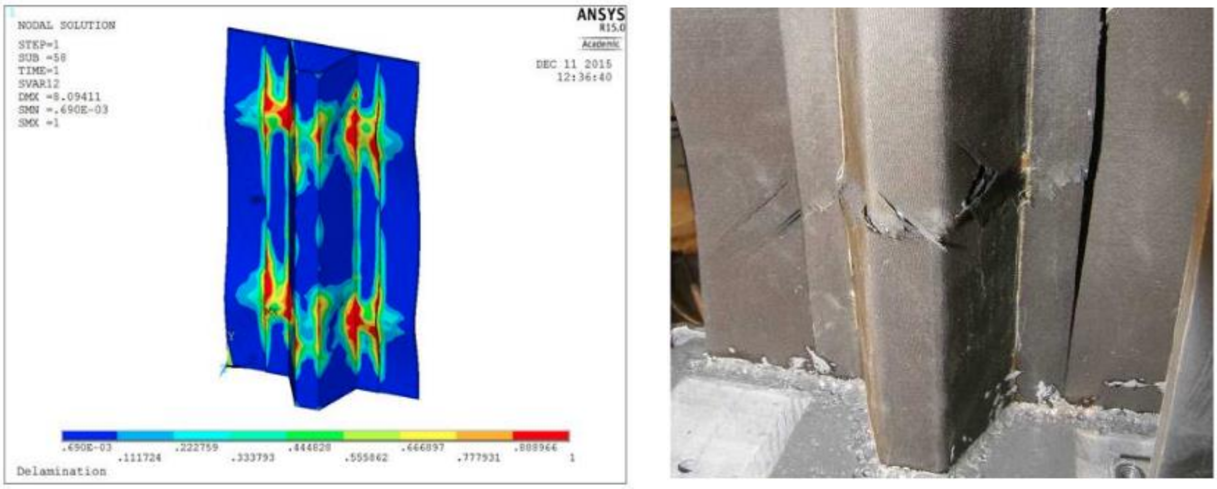

(c) (d)

Figure 4. Post-buckling progressive failure map: (a) fiber breakage, (b) matrix crack, (c) delamination and (d) experimental final failure [3].

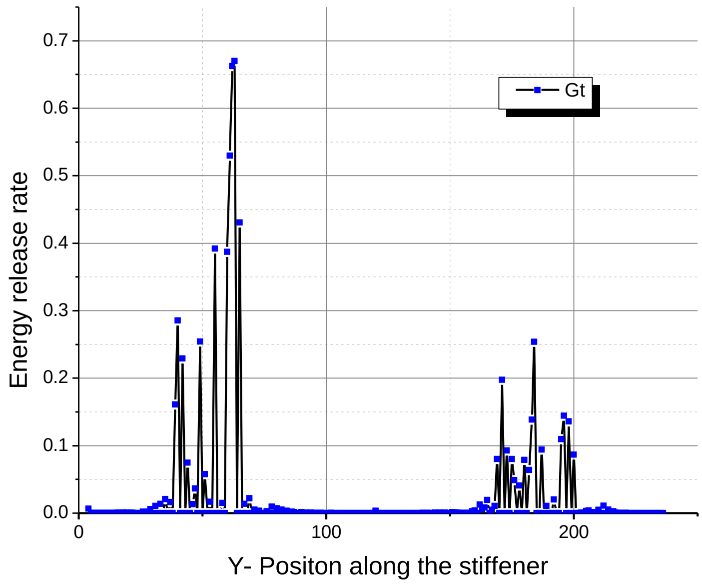

Figure 5. Energy release rate distribution along the stringer at 35kN

Failure initiation and propagation determined by using VCCT are predicted in post buckling region, the results shown in (fig.5) highlight the same critical area identified by progressive damage model. The energy distribution computed along the flange tip shows higher energy values at the maximum out of plane displacement, especially in the bottom region, which seems to be more the critical, and where the experimental failure are observed (fig. 4-d). The VCCT shows also that the contribution of the first mode G_I is the most important compared to other modes. This can be explained by the out of plane stress generated by high deflection where the skin tends to peel away from the stiffener and cause delamination onset.

5. Investigation of damage modes in two delta stringers panel
5.1 Geometry definition

In this section, a CFRP stiffened panel with two delta shape stringer provided by our industrial partner is investigated under compression loading. The test panel had 580 mm length by 382mm width and made with unidirectional material Cytec HTS 977-2. The skin consist of 12 plies with symmetric stacking sequence of $[90/45/-45/0/-45/45]_s$for a total thickness of 1.644mm. The stringers are composed of a 10-ply quasi-isotropic laminate with a stacking sequence of $[90/45/0/-45/0]_s$ which result of a total thickness of 1.35mm. The material properties and strength used in this model are presented in (Table 2).

Table 2. Material properties for two delta stringers panel

Mechanical properties	$\mathbf{E_{11}}$ (GPa)	$\mathbf{E_{22}=E_{33}}$ (MPa)	$\mathbf{G_{12}}$ (MPa)	$\mathbf{G_{23}=G_{13}}$ (MPa)	$\boldsymbol{\upsilon_{12}}$	$\boldsymbol{\upsilon_{23}}$	$\boldsymbol{\upsilon_{13}}$	
	148	9500	4500	3170	0.3	0.4	0.4	
Strength (MPa)	$\mathbf{X_T}$	$\mathbf{X_C}$	$\mathbf{Y_T}$	$\mathbf{Y_C}$	$\mathbf{Z_T}$	$\mathbf{Z_C}$	$\mathbf{S_{12}}$	$\mathbf{S_{23}=S_{13}}$
	2000	1500	50	150	100	253	150	41.5

5.2. Buckling behavior and damage scenario

The different phases of the panel response are illustrated in (fig. 6). Firstly the structure exhibits a linear response until 40kN with one single-wave out-of-plane deformation mode along the free edge of the skin. This phase is illustrated by configuration (A). A slight deviation is next observed at 40kN which corresponds to the apparition of the first buckling mode. This mode affects only the skin and still localized within the area between two stringers. Three, then four half-waves are observed successively in the middle of the panel and are presented by configuration B and C. By increasing loading, this deflection affects both panel sides around 62kN loading (configuration D). At 138 kN, the first buckling signs affecting the stringer are observed (E), despite this deformation stringer remain stable and still carrying loads. The final step is characterized by stringers collapse at 162 kN, where highly distorted elements are observed in both stringer webs (F).

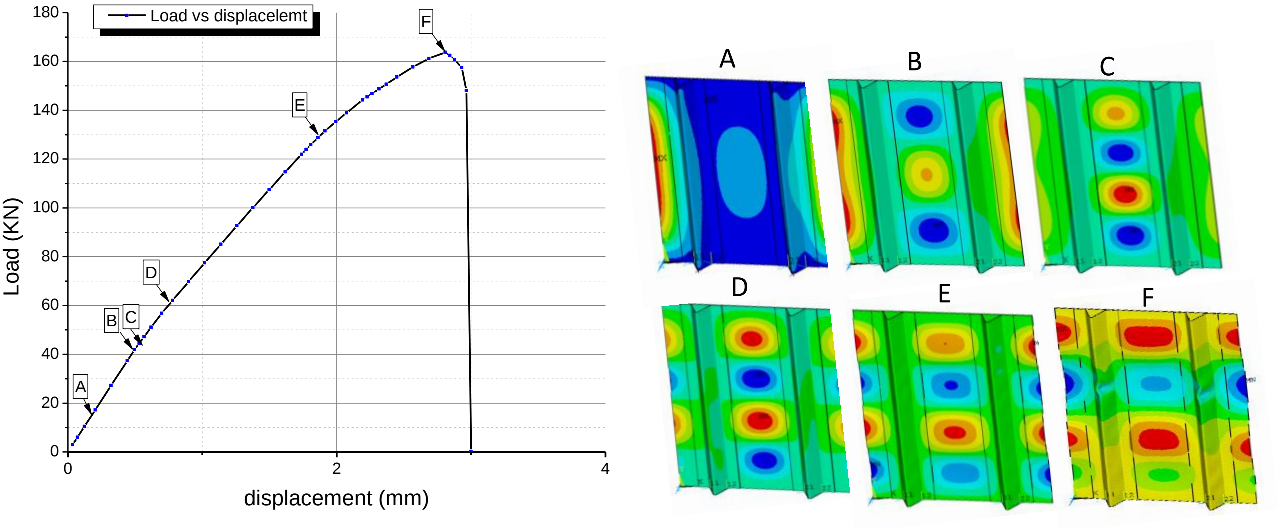

(a) (b)

Figure 6. Analysis of two stringer specimen: a) load-displacement curve; b) out-of-plane response.

In this geometry, damage failure is expected to happen in the region with the highest negative displacement located in the middle of the panel. Firstly, matrix cracks were observed just after the point D, matrix damage spreads and alter larger area before the apparition of the first fiber failure. In this case, almost all of fiber failures are still confined to the stiffener zone which provokes the final collapse of the panel. Figure 7, reports the three main failure modes observed in this panel prior the final collapse.

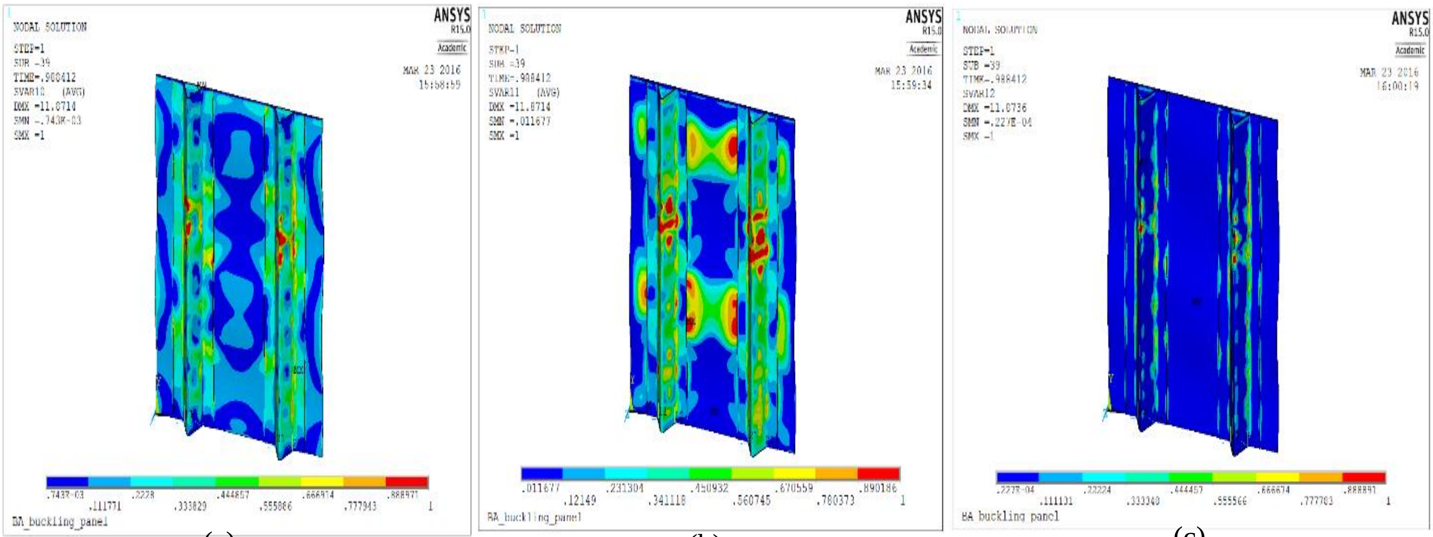

(a) (b) (c)

Figure 7: Post-buckling progressive failure map: (a) fiber breakage, (b) matrix cracking and (c) delamination

6. Conclusion

In this study, modeling and numerical prediction of failure modes, such as delamination, matrix cracking and fiber failure occurring in the post buckling stiffened panel was conducted based on progressive failure analysis (PFA). For this aim, an imbedded program using USERMAT subroutine was developed allowing to assess damage evolution and predict the final collapse. The proposed model is based on Olmedo [8] development where damage modes related to matrix, fiber and delamination criteria are examined for every loading step and appropriate degradation rules are applied.

This model was firstly applied with success on one simple plate with hole, where different failure modes were presented and delamination spread was compared to experimental results. Subsequently, one single stiffener panel was modeled under buckling loading, and the proposed damage model shows that it can reproduce the major damage modes involved throughout this process with good agreement as well as the final failure load despite the shift observed in the curve slope. In the last part of this study, large panel with two delta stiffeners was investigated. Different buckling phases were illustrated then the damage location and sequences are highlighted.

The progressive damage model proposed has shown promising results with efficient computing time for the different study cases. This approach can be considered as a reliable tool for damage tolerance study in large scale structures with complex behavior and various damage mode. Including major failure criteria, the proposed model could predict accurately the global response and estimate the final strength. It allows a wide understanding of the sequences behind damage mechanism involved throughout failure process which could be a valuable input in design stage.

Excerpt from ISBN 978-3-00-053387-7

Future work

This numerical investigation will be supported by experimental tests on two stringer panel using digital image correlation system for displacement and strain mapping. This step will allow a close monitoring of the panel behavior until final collapse and a better validation.

Acknowledgements

The author would like to acknowledge the Consortium of Research and Innovation in Aerospace in Quebec (CRIAQ), Natural Sciences and Engineering Research Council of Canada (NSERC), Bombardier Aerospace, L-3 MAS and MITACS for their funding.

References:

[1] E, Greenhalgh. M. H, Garcia. Fracture mechanisms and failure processes at stiffener run-outs in polymer matrix composite stiffened elements. *Composites Part A: Applied Science and Manufacturing,* volume 35, numéro 12, p. 1447-1458. 2004.

[2] M. M. Ratwani.: Effect of Damage on Strength and Durability. Rolling Hills Estates, CA 90274-4886 USA.2008.

[3] C. Bisagni, R. Vescovini and C.G. Dávila: Assessment of the Damage Tolerance of Postbuckled Hat-Stiffened Panels using Single-Stringer Specimens. *American Institute of Aeronautics and Astronautics*

[4] K. Ronald: Virtual crack closure technique: History, approach, and applications
National Institute of Aerospace, Hampton, Virginia 23666 Appl. Mech. Rev. 2004.

[5] G. Alfano and M.A. Crisfield. “Finite Element Interface Models for the Delamination Anaylsis of Laminated Composites: Mechanical and Computational Issues”. *International Journal for Numerical Methods in Engineering. Vol. 50. 1701-1736. 2001.*

[6] F.K Chang and K.Y Chang: A Progressive Damage Model for Laminated Composites Containing Stress Concentrations. *Journal of Composite Materials 21: 834-855. September 1987.*

[7] M. M. Shokrieh and L. B. Lessard: Progressive Fatigue Damage Modeling of Composite Materials, Part I: *Modeling Journal of Composite Materials, 34: 1056-1080. July 2000.*

[8] Á. Olmedo, C. Santiuste: On the prediction of bolted single-lap composite joints. *Composite Structures Volume 94, Issue 6, Pages 2110–2117, May 2012*

[9] Z. Hashin. Failure criteria for unidirectional fiber composites. *J Appl Mech; 47(2):329–34. 1980.*

[10] A. Puck, H. Schürmann. Chapter 3.7 - Failure analysis of FRP laminates by means of physically based phenomenological models. 2004.

[11] S. Pinho, C. Davila, P. Camanho, L. Iannucci, P. Robinson. Failure models and criteria for FRP under in-plane or three-dimensional stress states including shear non-linearity. *NASA/TM-213530. 2005.*

[12] Abaqus Analysis User’s Manual, Simulia; 2011.

[13] E. Pietropaoli: Progressive Failure Analysis of Composite Structures Using a Constitutive Material Model (USERMAT) Developed and Implemented in ANSYS. *Applied Composite Materials, Volume 19, Issue 3, pp 657-668, June 2012.*

Excerpt from ISBN 978-3-00-053387-7